Preparation and Microwave Absorption Properties of Melt-Spun Nd$_2$Co$_{17}$ Alloys with Different Post-Treatment Processes

XIN GAO,[1] GUOZHI XIE ●,[1,3] NINGYAN XIE,[1] LINGLI ZHAO,[2] XUEYING ZHANG,[2] LI YANG,[2] and JING CHEN[1]

1.—College of Electronic and Optical Engineering & College of Microelectronics, Nanjing University of Posts and Telecommunications, Nanjing 210023, People's Republic of China. 2.—College of Telecommunications and Information Engineering, Nanjing University of Posts and Telecommunications, Nanjing 210023, People's Republic of China. 3.—e-mail: guozhixie@njupt.edu.cn

Nd$_2$Co$_{17}$ alloy particles were prepared by melt-spinning and high-energy ball-milling techniques. Vacuum heat treatment or crushing was added during the fabrication period to obtain absorbing powders. The microstructure and electromagnetic properties of the absorbing powders were studied. The electromagnetic parameters were investigated using an Agilent vector network analyzer. The size and thickness of the crushed alloy powders was distinctly decreased compared with that of the uncrushed sample. The reduced size and thickness of alloy powers can significantly enhance electromagnetic matching for absorbing powders. Consequently, the microwave absorption properties of the crushed alloys were significantly improved. The reflection loss (RL), which is based on transmission line theory, shows that the vacuum heat treatment sample had an RL peak in the C-band. However, the crushed sample had an RL peak between the C-band and the X-band. The minimum RL value of −8.1 dB was obtained at 8.2 GHz for the crushed Nd$_2$Co$_{17}$ alloy, and the absorption bandwidth at less than −5 dB reached 9.4 GHz. In contrast, the RL peak of the Nd$_2$Co$_{17}$ alloys without post-treatment was located in the S-band. These results prove that proper post-treatment is the key to regulating electromagnetic matching, whereby optimal microwave absorption properties of the alloys can be obtained in different bands.

Key words: Melt-spinning, post-treatment, microwave absorbing, electromagnetic matching

INTRODUCTION

Over the past few decades, various types of gigahertz electromagnetic wave devices have been widely used.[1] Therefore, electromagnetic interference (EMI) and electromagnetic (EM) radiation pollution have become more serious, creating an urgent need for a solution.[2] EMI and EM radiation will not only cause serious interference to the electronic control system, but will also endanger human health.[3] In research efforts to weaken and eliminate EMI and EM radiation, microwave-absorbing materials have gradually become the focus of attention.[4]

Metal magnetic materials such as iron, cobalt, nickel and their alloy particles have a high Snoek limit at gigahertz frequencies and satisfactory saturation magnetization, which makes them exhibit good microwave absorption properties.[5] However, it is well known that the shape and size also play an important role in the microwave absorption performance of metal magnetic materials.[6–9] Researchers have reported high reflection losses at 1–8 GHz for micron-sized cobalt powders.[10] Composites containing FeCo particles can be applied as thin, wideband microwave absorbers.[11] Cobalt particles have been

found to present good microwave absorption properties in targeting bands over a wide temperature range due to their multiple crystal structures, large saturation magnetization and high Curie temperature (1130°C).[12] The main disadvantage of metal magnetic alloys is their high electrical conductivity, the consequence of which is the degradation of the chemical composition of metal alloys, namely oxidation, over time.[13,14] The oxidation behavior may be harmful to their magnetic properties and microwave absorption performance. However, improved oxidation resistance can be obtained in Co-based superalloys.[15]

Doping is an effective method for improving the magnetic and microwave absorption properties of metal magnetic materials, and the choice of dopant type and location is critical.[16,17] Rare earth (RE) alloys and compounds with the unique 3D-4f interactions between transition metals can improve electromagnetic wave absorbing performance, widen the bandwidth and reduce matching-thickness.[18] Therefore, rare earth is a good choice as an alloy dopant. Doped relatively low RE elements in metal soft magnetic materials can obtain better matching frequency.[19] Doping RE in ferrite materials is an efficient method to increase the magnetic and microwave-absorbing ability of the materials.[20] Wang reported that doping of Sm^{3+} in a $BaCo_2Fe_{16}O_{27}$ alloy could greatly improve the composite permeability.[21]

In this study, Nd_2Co_{17} metal soft magnetic material was prepared by rapid quenching technology. The effects of crushing and vacuum heat treatment on the microwave absorption properties for the milled Nd_2Co_{17} alloys were studied.

EXPERIMENT

Nd_2Co_{17} alloys were prepared using high-purity Nd (99.8 wt.%) and Co (99.8 wt.%) metals. Homogeneous alloys were obtained by arc-melting these ingots three times, and then melt-spinning in a molybdenum wheel at a speed of 50 m/s in an argon atmosphere. After quenching, three different post-treatment methods were applied to the sample. Sample #1 was ground by a ball mill for 2 h at a speed of 500 r/min; the material of the ball was E52100 with a diameter of 8 mm. The ball-to-power weight ratio was set at 10:1 throughout the experimental process. Sample #2 was subjected to vacuum heat treatment at 400°C before ball milling. Sample #3 was crushed and then ball-milled; the mixtures were crushed for 20 min to obtain fine powders. The numbers of Nd_2Co_{17} alloys under different post-treatment methods are shown in Table I.

The microstructures of the samples treated by different processes were measured using an S-3400 scanning electron microscope (SEM; Hitachi, Ltd., Japan). The coaxial annular samples with 7.0 mm outer diameter, 3.04 mm inner diameter and 3–

Table I. The numbers of Nd_2Co_{17} alloys under different post-treatment methods

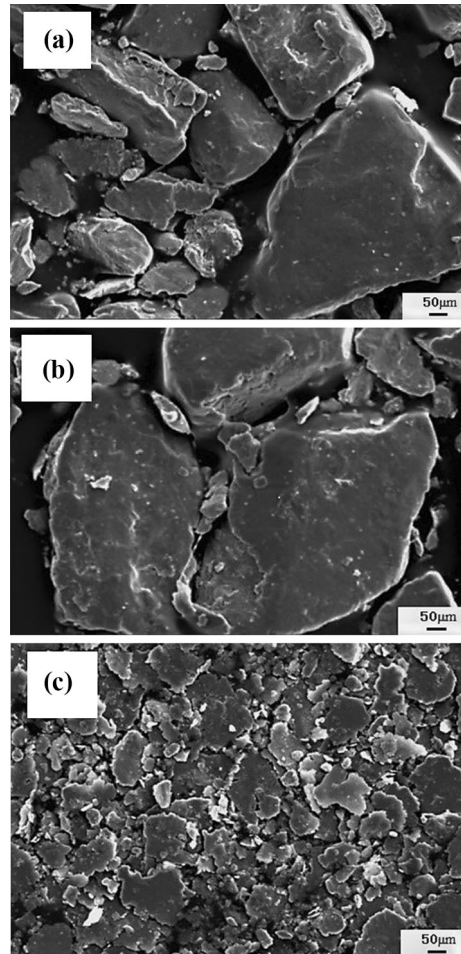| Sample no.	Treatment method
1	As milled
2	Vacuum heat treatment + as milled
3	Crushing + as milled

Fig. 1. SEM images of Nd_2Co_{17} alloy samples under different post-treatment methods: (a) as milled, (b) vacuum heat treatment + as milled, (c) crushing + as milled.

4 mm thickness were prepared by mixing the ground Nd_2Co_{17} alloy powder with 15 wt.% paraffin wax. The electromagnetic parameters of the samples were measured by a microwave vector network analyzer (Agilent PNA8363B) based on a coaxial line method in the 2–18 GHz band. The reflection loss of the samples processed using different post-treatment methods was calculated based on transmission line theory.

RESULTS AND DISCUSSION

Figure 1 shows the SEM images of the rapidly quenched Nd_2Co_{17} magnetic alloy with different post-treatment methods. From Fig. 1a, it can be seen that the flake structure of the as-milled powder is not obvious, the diameter varies from 10 μm to 50 μm, and the thickness is relatively large, about 10 μm. Compared with Fig. 1a, the micro-morphology of Fig. 1b shows no obvious change, which indicates that vacuum heat treatment has little effect on the micro-morphology of the material. Figure 1c shows the crushed sample with a post-milling process. It can be easily observed that the alloy powder presents a flat sheet structure. The thickness of the alloy powder is about 1 μm less than that of the former, and the average particle diameter is less than 20 μm. The flat flake structure gives the powder an anisotropy that allows it to exceed the Snoek limit, improving the microwave absorption properties.[22,23]

Figure 2 shows the complex permittivity of Nd_2Co_{17} samples treated by different processing methods. In Fig. 2a, the ε' values decrease slowly with the increase in frequency, indicating good consistency with the frequency dispersion. As shown in Fig. 2b, in the 2–11 GHz range, the ε'' of sample #1 decreases sharply with the increase in frequency, and the sample curve is always at the top. The ε'' of sample #2 decreases relatively as a whole. The appearance of grain boundaries may be the reason for the decrease in complex permittivity after annealing, which reduces space charge polarization and leads to electron scattering.[24] Sample #3 maintains a relatively stable value and is always the smallest. The inner stress and defect generated in the process of crushing may explain this result.[25] The absorption properties of materials are greatly affected by the complex permittivity. For magnetic alloy materials, the complex permeability is much smaller than the complex permittivity, and reducing complex permittivity can effectively reduce the skin effect of materials, thus achieving impedance matching in a broader frequency range.[26]

Figure 3 shows the complex permeability of the Nd_2Co_{17} samples relative to frequency. The relatively low complex permeability for all samples may occur for the following two reasons: (1) The high frequency response of the complex permeability of soft magnetic materials is significantly affected by the magnetic resonance at high frequencies and
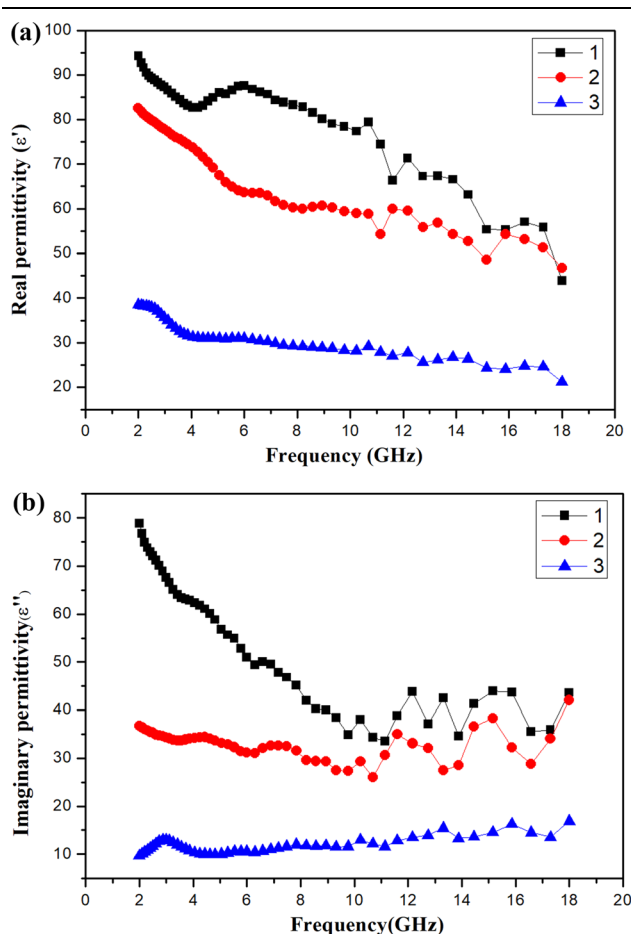

Fig. 2. The complex permittivity of Nd₂Co₁₇ alloy samples under different post-treatment methods.
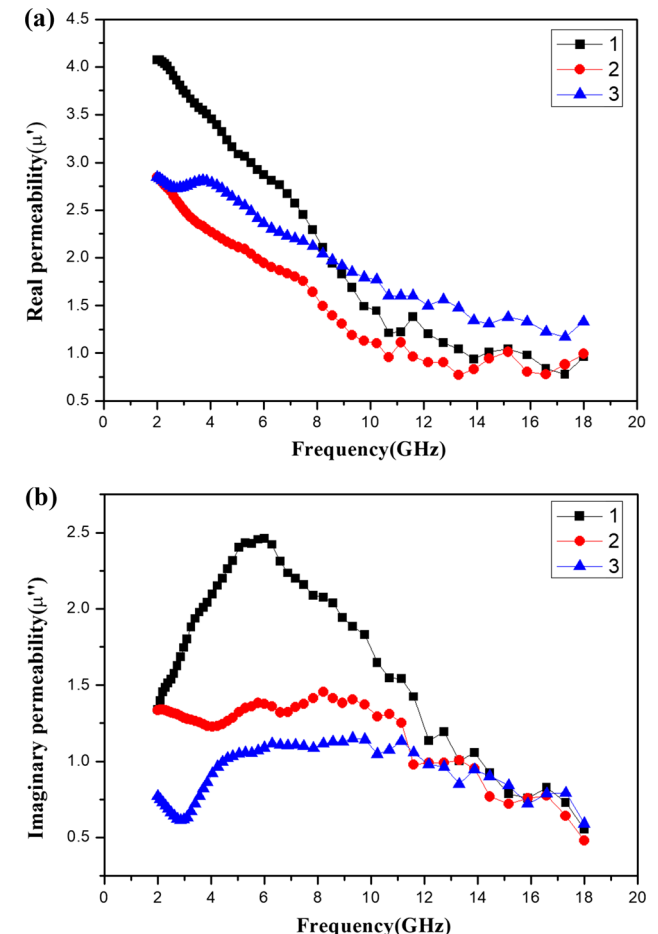

Fig. 3. The complex permeability of Nd₂Co₁₇ alloy samples under different post-treatment methods.

eddy current losses.[27] Therefore, the weak magnetic anisotropy field of the soft magnetic alloy [28–30] results in lower permeability. (2) The penetration of oxygen into the crystallites of the alloy and the formation of oxides throughout the volume causes a serious reduction in the initial magnetic properties of the alloys.[31,32] At 2 GHz, all samples have the largest μ', which then continues to decrease as the frequency increases up to 18 GHz. The μ'' value of sample #1 increases steadily at frequencies of 2– 6 GHz, then decreases at frequencies of 6–18 GHz. The jump of μ'' for the sample may occur for the following two reasons: (1) the exchange coupling between the fine grains,[33,34] and (2) the flake-like-shaped uniform particles of the alloy powder, which can produce multi-resonance consisting of broad resonance bands.[35] Ma et al. also reported that the jump in μ'' is mainly attributable to the natural resonance originating from the shape anisotropy and magnetocrystalline anisotropy.[36] However, the other two samples remain stable until 11 GHz, and then show good consistency with the frequency dispersion. The values of permeability obtained in sample #3 are more stable than the other two samples, which can benefit a wider microwave absorption bandwidth.[37] The complex permeability is enhanced with the increase in the aspect ratio (the ratio of the diameter and the thickness is defined as the aspect ratio).[38] It can be seen from the SEM images that the aspect ratio of sample #3 is the smallest. This results in the lowest complex permeability for sample #3.

Figure 4 shows the tangent values of dielectric loss angle ($\tan \delta_\varepsilon = \varepsilon''/\varepsilon'$) and the tangent values of magnetic loss angle ($\tan \delta_\mu = \mu''/\mu'$) for Nd_2Co_{17} samples with different post-treatment methods. In Fig. 4a, as the frequency increases, the tangent of dielectric loss angle of sample #1 first decreases and then increases, while that of samples #2 and #3 increases with increasing frequency. This indicates that the dielectric loss ability of the samples is changed to some extent by crushing and vacuum heat treatment. As shown in Fig. 4b, the tangent values of magnetic loss for the three samples increase at first and then decrease. In contrast, the $\tan \delta_\mu$ of sample #3 is obviously lower but relatively stable. In general, larger $\tan \delta_\varepsilon$ and $\tan \delta_\mu$ indicate that the sample will have excellent electromagnetic wave absorption performance within the whole frequency range.[39] Among all samples, larger $\tan \delta_\varepsilon$ and $\tan \delta_\mu$ are achieved for sample #1, but the $\tan \delta_\mu$ value is the largest and the $\tan \delta_\varepsilon$ value the smallest, which leads to poor impedance matching. It can be seen from the figure that sample #3 treated by crushing is able to achieve impedance matching more easily, and in this way better microwave absorption can be obtained.

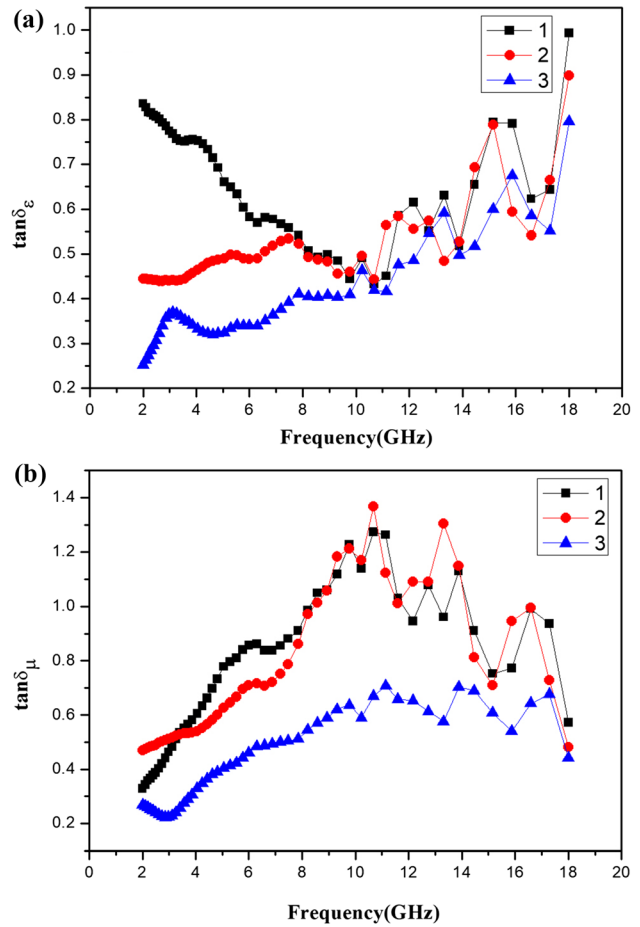The coefficient of electromagnetic matching δ can be calculated from the following equations[40]:

Fig. 4. Tangent values of dielectric loss angle and magnetic loss angle for Nd_2Co_{17} alloy samples under different post-treatment methods.

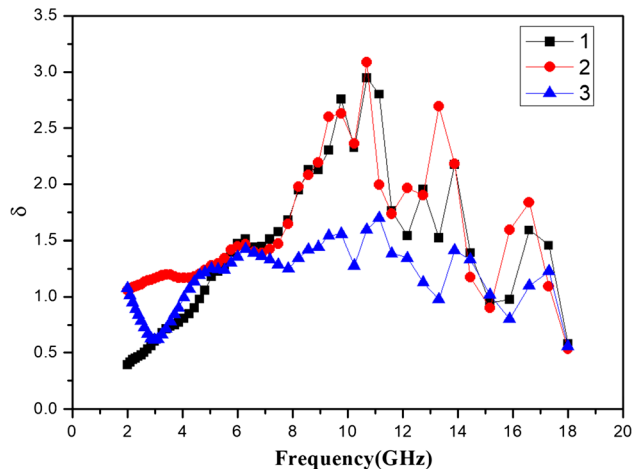Fig. 5. The coefficient of electromagnetic matching (δ) of Nd_2Co_{17} alloy samples under different post-treatment methods as a function of frequency.

$$\delta = \frac{\mu''/\varepsilon''}{\mu'/\varepsilon'} = \frac{\mu''\varepsilon'}{\mu'\varepsilon''}. \tag{1}$$

Preparation and Microwave Absorption Properties of Melt-Spun Nd_2Co_{17} Alloys with Different Post-Treatment Processes

1171

According to the generalized electromagnetic matching theory, when δ approaches 1, the electromagnetic matching performance is good. Figure 5 shows the values of δ for different post-treatment methods. It can be clearly seen that, among the three samples, the δ value of sample #3 is closest to a constant. Therefore, better electromagnetic matching was achieved in the crushed Nd_2Co_{17} alloy, which enhanced microwave absorption in another way.

The microwave absorption performance of an absorber depends on two important parameters: complex permittivity ($\varepsilon = \varepsilon' - j\varepsilon''$) and complex permeability ($\mu = \mu' - j\mu''$). The terms ε' or μ' are associated with energy storage, and ε'' or μ'' refers to the energy dissipation from dipolar, resonance, conduction and relaxation mechanisms.[41] The closer the values of ε and μ, the greater the reflection loss and the lower reflection of the electromagnetic wave that will be achieved.[42]

According to transmission line theory, when the normal incident electromagnetic wave is at a given frequency and absorber thickness, reflection loss can be calculated according to the following equation[25,43]:

$$Z_0 = \sqrt{\frac{\mu_0}{\varepsilon_0}} \qquad (2)$$

$$Z_{in} = \sqrt{\frac{\mu}{\varepsilon}} \tan h \left(j \frac{2\pi fd}{c} \right) \sqrt{\mu\varepsilon} \qquad (3)$$

$$RL = 20 \lg \left| \frac{Z_{in} - Z_0}{Z_{in} + Z_0} \right|. \qquad (4)$$

Here, Z_0 is the impedance of air, Z_{in} is the input impedance of the absorber, c is the velocity of light, d is the thickness of the absorber, f is the frequency of 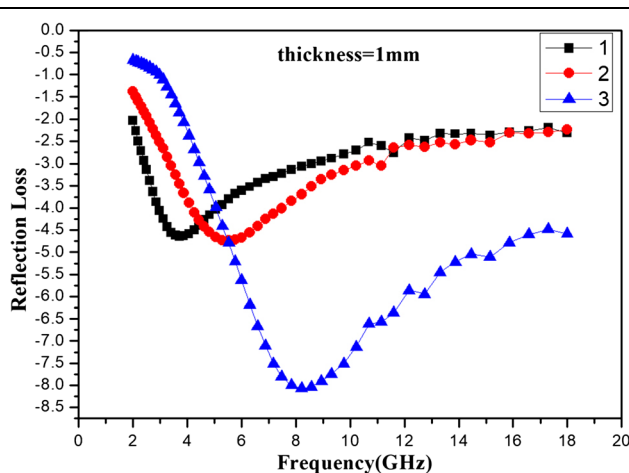the electromagnetic wave, μ_0 and ε_0 are the permeability and permittivity of air, respectively, and μ and ε are the complex permeability and complex permittivity of the absorber, respectively. Figure 6 shows the reflection loss of the Nd_2Co_{17} alloy sample under different treatment processes, which clearly reveals the effect of the different post-treatment methods on reflection loss. For samples #1 and #2, the minimum reflection losses are -4.6 dB at 3.7 GHz and -4.8 dB at 5.5 GHz, respectively. The as-spun sample has a reflection loss peak in the S-band, while that of the sample with vacuum heat treatment is in the C-band. Sample #3 achieved the lowest reflectivity value of -8.1 dB at 8.2 GHz. The crushed sample has the reflection loss peak between the C-band and X-band, and the absorption frequency bandwidth less than -5 dB reaches 9.4 GHz. From Fig. 6, it can be seen that the resonance frequency of the samples after post-treatment was shifted to a high frequency, which may be due to the change in shape anisotropy and the increase in internal anisotropic field.[44–46]

CONCLUSIONS

The microstructure and microwave properties of melt-spun Nd_2Co_{17} alloy powders using different post-treatment methods were studied in this paper. Vacuum heat treatment had little effect on the micro-morphology of the material. However, the size and thickness of the crushed alloy powers were significantly reduced compared with those by vacuum heat treatment. The crushed alloy powders were found to present a flat sheet structure, which helped to improve the electromagnetic matching of the crushed Nd_2Co_{17} alloy. The minimum reflection loss of the crushed Nd_2Co_{17} alloy reached -8.1 dB at 8.2 GHz with a thickness of 1 mm. In addition, the absorption bandwidth (RL < -5 dB) was achieved within a range of 5.7–15.1 GHz, which may be applied to the C- and X-bands. Meanwhile, the reflection loss peak by vacuum heat treatment was located in the C-band. In contrast, the as-spun sample with ball milling had a reflection loss peak in the S-band. These results show that proper post-treatment is the key to regulating electromagnetic matching, whereby the optimal microwave absorption properties of the alloys can be obtained in different bands.

ACKNOWLEDGMENTS

Fig. 6. Reflection loss of Nd_2Co_{17} alloy samples under different post-treatment methods.

REFERENCES

1. H.B. Yi, F.S. Wen, L. Qiao, and F.S. Li, *J. Appl. Phys.* 106, 103922 (2009).
2. S. Geetha, K.K. Satheesh Kumar, C.R.K. Rao, M. Vijayan, and D.C. Trivedi, *J. Appl. Polym. Sci.* 112, 2073 (2009).
3. G.Z. Shen, Y.W. Xu, B. Liu, P. Du, Y. Li, J. Zhu, and D. Zhang, *J. Alloys Compd.* 680, 553 (2016).

4. C.K. Zhang, J.J. Jiang, S.W. Bie, L. Zhang, L. Miao, and X.X. Xu, *J. Alloys Compd.* 527, 71 (2012).
5. T. Liu, P.H. Zhou, J.L. Xie, and L.J. Deng, *J. Appl. Phys.* 110, 033918 (2011).
6. S.S. Grabchikov, A.V. Trukhanov, S.V. Trukhanov, I.S. Kazakevich, A.A. Solobay, V.T. Erofeenko, N.A. Vasilenkov, O.S. Volkova, and A. Shakin, *J. Magn. Magn. Mater.* 398, 49 (2016).
7. A.V. Trukhanov, S.S. Grabchikov, A.A. Solobai, D.I. Tishkevich, S.V. Trukhanov, and E.L. Trukhanova, *J. Magn. Magn. Mater.* 443, 142 (2017).
8. T.I. Zubar, S.A. Sharko, D.I. Tishkevich, N.N. Kovaleva, D.A. Vinnik, S.A. Gudkova, E.L. Trukhanova, E.A. Trofimov, S.A. Chizhik, L.V. Panina, S.V. Trukhanov, and A.V. Trukhanov, *J. Alloys Compd.* 748, 970 (2018).
9. T.I. Zubar, V.M. Fedosyuk, A.V. Trukhanov, N.N. Kovaleva, K.A. Astapovich, D.A. Vinnik, E.L. Trukhanova, A.L. Kozlovskiy, M.V. Zdorovets, A.A. Solobai, D.I. Tishkevich, and S.V. Trukhanov, *J. Electrochem. Soc.* 166, D173 (2019).
10. C.K. He, S.K. Pan, L.C. Cheng, X. Liu, and Y.J. Wu, *J. Rare Earth* 33, 271 (2015).
11. Y. Zare, M.H. Shams, and M. Jazirehpour, *J. Alloys Compd.* 717, 294 (2017).
12. N. Chen, J.T. Jiang, Y. Yuan, C. Liu, C.Y. Xu, and L. Zhen, *J. Magn. Magn. Mater.* 421, 368 (2017).
13. A.V. Trukhanov, L.V. Panina, S.V. Trukhanov, V.A. Turchenko, and M. Salem, *Chin. Phys. B* 25, 016102 (2016).
14. S.V. Trukhanov, A.V. Trukhanov, V.G. Kostishyn, L.V. Panina, V.A. Turchenko, I.S. Kazakevich, A.V. Trukhanov, E.L. Trukhanova, V.O. Natarov, and A.M. Balagurov, *J. Magn. Magn. Mater.* 426, 554 (2017).
15. H.-Y. Yan, V.A. Vorontsov, and D. Dye, *Intermetallics* 48, 44 (2014).
16. V. Turchenko, A. Trukhanov, S. Trukhanov, M. Balasoiu, and N. Lupu, *J. Magn. Magn. Mater.* 477, 9 (2019).
17. A.V. Trukhanov, M.A. Darwish, L.V. Panina, A.T. Morchenko, V.G. Kostishyn, V.A. Turchenko, D.A. Vinnik, E.L. Trukhanova, K.A. Astapovich, A.L. Kozlovskiy, M. Zdorovets, and S.V. Trukhanov, *J. Alloys Compd.* 791, 522 (2019).
18. Z.Q. Qiao, S.K. Pan, J.L. Xiong, L.C. Cheng, Q.R. Yao, and P.H. Lin, *J. Magn. Magn. Mater.* 423, 197 (2017).
19. H. Wang, G.Z. Xie, N.Y. Xie, L.J. Ye, J.W. Chen, and J. Chen, *J. Mater. Sci.* 30, 401 (2019).
20. Z.Y. Zhang, X.X. Liu, X.J. Wang, Y.P. Wu, and R. Li, *J. Alloys Compd.* 525, 114 (2012).
21. L.X. Wang, J. Song, Q.T. Zhang, X.G. Huang, and N.C. Xu, *J. Alloys Compd.* 481, 863 (2009).
22. J.L. Snoek, *Nature* 160, 90 (1947).
23. W.F. Yang, L. Qiao, J.Q. Wei, Z.Q. Zhang, T. Wang, and F.S. Li, *J. Appl. Phys.* 107, 033913 (2010).
24. J.H. He, W. Wang, A.M. Wang, and J.G. Guan, *J. Magn. Magn. Mater.* 324, 2902 (2012).
25. G.Z. Xie, X.L. Song, B.S. Zhang, D.M. Tang, Q. Bian, and H.X. Lu, *Powder Technol.* 210, 220 (2011).
26. J. Li, G.Z. Xie, P.C. Ji, J. Qu, J.W. Chen, and J. Chen, *J. Magn. Magn. Mater.* 443, 85 (2017).
27. S. Ohnuma, H.J. Lee, N. Kobayashi, H. Fujimori, and T. Masumoto, *IEEE Trans. Magn.* 37, 2251 (2001).
28. A.V. Trukhanov, V.G. Kostishyn, L.V. Panina, V.V. Korovushkin, V.A. Turchenko, P. Thakur, A. Thakur, Y. Yang, D.A. Vinnik, E.S. Yakovenko, LYu Matzui, E.L. Trukhanova, and S.V. Trukhanov, *J. Alloys Compd.* 754, 247 (2018).
29. A.V. Trukhanov, S.V. Trukhanov, V.G. Kostishyn, L.V. Panina, V.V. Korovushkin, V.A. Turchenko, D.A. Vinnik, E.S. Yakovenko, V.V. Zagorodnii, V.L. Launetz, V.V. Oliynyk, T.I. Zubar, D.I. Tishkevich, and E.L. Trukhanova, *J. Magn. Magn. Mater.* 462, 127 (2018).
30. A.V. Trukhanov, L.V. Panina, S.V. Trukhanov, V.G. Kostishyn, V.A. Turchenko, D.A. Vinnik, T.I. Zubar, E.S. Yakovenko, LYu Macuy, and E.L. Trukhanov, *Ceram. Int.* 44, 13520 (2018).
31. S.V. Trukhanov, I.O. Troyanchuk, N.V. Pushkarev, and H. Szymczak, *JETP* 95, 308 (2002).
32. S.V. Trukhanov, I.O. Troyanchuk, A.V. Trukhanov, I.M. Fita, A.N. Vasil'ev, A. Maignan, and H. Szymczak, *JETP Lett.* 83, 33 (2006).
33. T. Maeda, S. Sugimoto, T. Kagotani, N. Tezuka, and K. Inomata, *J. Magn. Magn. Mater.* 281, 195 (2004).
34. M. Itoh, K. Nishiyama, F. Shogano, T. Murota, K. Yamamoto, M. Sasada, and K. Machida, *J. Alloys Compd.* 451, 507 (2008).
35. L.J. Deng, P.H. Zhou, J.L. Xie, and L. Zhang, *J. Appl. Phys.* 101, 103916 (2007).
36. Z. Ma, Q.F. Liu, J. Yuan, Z.K. Wang, C.T. Cao, and J.B. Wang, *Phys. Status Solidi B* 249, 575 (2012).
37. X.Q. Shen, F.Z. Song, J. Xiang, M.Q. Liu, Y.W. Zhu, and Y.D. Wang, *J. Am. Ceram. Soc.* 95, 3863 (2012).
38. Y.B. Feng and T. Qiu, *J. Magn. Magn. Mater.* 324, 2528 (2012).
39. G. Li, G.G. Hu, H.D. Zhou, X.J. Fan, and X.G. Li, *Mater. Chem. Phys.* 75, 101 (2002).
40. Z.L. Zhang, Z.J. Ji, Y.P. Duan, S.C. Gu, and J.B. Guo, *J. Mater. Sci.* 24, 968 (2013).
41. F.B. Meng, H.G. Wang, F. Huang, Y.F. Guo, Z.Y. Wang, D. Hui, and Z.W. Zhou, *Compos. Part. B* 137, 260 (2018).
42. Q.M. Su, G. Zhong, J. Li, G.H. Du, and B.S. Xu, *Appl. Phys. A* 106, 59 (2012).
43. B.S. Zhang, G. Lu, Y. Feng, J. Xiong, and H.X. Lu, *J. Magn. Magn. Mater.* 299, 205 (2006).
44. S.V. Trukhanov, A.V. Trukhanov, V.G. Kostishyn, L.V. Panina, A.V. Trukhanov, V.A. Turchenko, D.I. Tishkevich, E.L. Trukhanova, V.V. Oleynik, O.S. Yakovenko, L.Y. Matzui, and D.A. Vinnik, *J. Magn. Magn. Mater.* 442, 300 (2017).
45. S.V. Trukhanov, A.V. Trukhanov, V.G. Kostishyn, L.V. Panina, A.V. Trukhanov, V.A. Turchenko, D.I. Tishkevich, E.L. Trukhanova, O.S. Yakovenko, and L.Y. Matzui, *Dalton Trans.* 46, 9010 (2017).
46. S.V. Trukhanov, A.V. Trukhanov, V.G. Kostishyn, L.V. Panina, A.V. Trukhanov, V.A. Turchenko, D.I. Tishkevich, E.L. Trukhanova, O.S. Yakovenko, L.Y. Matzui, D.A. Vinnik, and D.V. Karpinsky, *J. Phys. Chem. Sol.* 111, 142 (2017).